IEEE Access
Multidisciplinary | Rapid Review | Open Access Journal

Received March 11, 2021, accepted April 20, 2021, date of publication April 23, 2021, date of current version May 17, 2021.

Digital Object Identifier 10.1109/ACCESS.2021.3075318

Simulation Analysis of the Electromagnetic Force Distribution and Formability Parameters for Sheet Metal Electromagnetic Bulging Using a New Magnetic Field Shaper

LI QIU[1,2], (Member, IEEE), WEIYE WU[1], AHMED ABU-SIADA[3], (Senior Member, IEEE), BIN WANG[1], WANG ZHANG[1], XI TIAN[1], AND CHENGLIN WANG[1]

[1]College of Electrical Engineering and New Energy, China Three Gorges University, Yichang 443002, China
[2]Hubei Provincial Key Laboratory of Operation and Control of Cascade Hydropower Stations, Yichang 443002, China
[3]Discipline of Electrical and Computer Engineering, Curtin University, Perth, WA 6102, Australia

Corresponding author: Chenglin Wang (1361145341@qq.com)

This work was supported in part by the National Natural Science Foundation of China under Grant 51877122 and Grant 51707104, and in part by the Research Fund for Excellent Dissertation of China Three Gorges University under Grant 2019SSPY065.

ABSTRACT While electromagnetic forming of aluminum alloy sheet has gained several advantages, the uneven radial deformation of the sheet is still one of the main drawback of this technology that calls for reliable and cost-effective solution. Aiming at this point, this paper presents an electromagnetic bulging system equipped with a new magnetic field shaper placed between the driving coil and the object sheet to modulate the distribution of the induced eddy current in the sheet, and hence regulating the distribution of the electromagnetic force to achieve more uniform deformation. A finite element electromagnetic-structure 2D coupling model simulating this process is developed and the effects of workpiece geometry and deformation speed on the circuit, magnetic field and structure field are considered. The coupling between the electric circuit and magnetic field; magnetic field and workpiece deformation is realized to simulate the actual system of thin plate electromagnetic bulging. The performance of the proposed system is compared with that of the traditional system through investigating the profiles of the induced eddy current, electromagnetic force and forming effect. Simulation results show that the uniformity of sheet metal forming is improved by using the proposed magnetic field shaper, and the maximum uniform deformation area is increasing from 32.1 mm to 73.8 mm, which stimulates more industrial applications of sheet metal electromagnetic forming.

INDEX TERMS Electromagnetic forming, magnetic field shaper, deformation uniformity, electromagnetic force, sheet metal bulging.

I. INTRODUCTION

Electromagnetic forming is a non-contact high-speed pulse forming technology that can provide improved the forming limit of materials than traditional machining [1]–[6]. Based on the nature of the object, the electromagnetic forming is categorized into tube or sheet processing [7]–[9]. Much attention was given in the literature to improve the uniformity of tube electromagnetic bulging. For example, in [10], a concave coil is used to load the tube. Reported results show that the electromagnetic force distribution generated by the proposed concave coil can effectively improve the uniformity of axial forming of the tube however, the coil assembling is complicated. In [11], a convex coil could achieve a uniform length of tube axial deformation 4.7 times of that achieved by a traditional driving coil. Ref. [12] presented a method that employs a concave driving coil to weaken the radial electromagnetic force in the middle of the tube and hence improving the tube-forming uniformity. A criterion of deformation homogeneity was proposed in [13] to quantify the forming uniformity of tube based on using small coils to induce individual eddy currents in the upper, middle and lower parts of the tube which resulted in improved pipe uniformity. An auxiliary coil for tube bulging is proposed in [14] to weaken the radial

The associate editor coordinating the review of this manuscript and approving it for publication was Xiaokang Yin.

electromagnetic force at tube ends and improve the forming uniformity.

On the other hand research on sheets electromagnetic bulging uniformity did not receive as much attention as the tube bulging. In [15], a uniform pressure coil is proposed to help the center of the sheet deform uniformly. In [16], a local electromagnetic force loading method is presented in which the local electromagnetic force has an obvious effect on the end of the sheet, and a little impact on the middle part to enhance its formability.

In addition to directly forming the workpiece with the driving coil, it is common to include a device named field shaper to adapt the electromagnetic force distribution [16]. In [17], a 3D model is developed to analyze the performance of an electromagnetic forming system equipped with a magnetic field shaper. Analysis reveals that by changing the structure parameters of the magnetic field shaper, the electromagnetic force distribution can be regulated. An electromagnetic welding system based on magnetic concentrator to improve the uniformity of the magnetic field and the electromagnetic force distribution is presented in [18]. Ref. [19] presented an experimental test to study the influence of the electromagnetic magnetic field shaper geometry on the final contour of the bulged tube. Also, the influence of different magnetic field shaper geometry on the final forming was studied in [20] through simulation and experimental analyses. In [22], a tube bulging technology based on magnetic field shaper is presented and the results show that the concave radial electromagnetic force generated by the magnetic field shaper can weaken the uneven deformation at the middle part of the tube.

Obviously, changing the structure and position of coils can change the magnetic field distribution, thus changing the level and distribution of the electromagnetic force and improving the forming uniformity of the workpiece. However, in the free bulging of sheet metal, there are few methods to improve the forming uniformity. Furthermore, while the magnetic field shaper is introduced in the literature, it is usually used to concentrate the electromagnetic force at specific regions of the sheet, without giving much attention to improve the entire sheet forming uniformity through a proper design for the magnetic field shaper. As such, this paper is aimed at filling this research gap by presenting a new magnetic field shaper-based method to improve the forming uniformity of sheet metals. The geometric parameters of the magnetic field shaper are analyzed through its impact on the forming uniformity of sheet metal. The performance of the proposed system is also compared with that of a traditional electromagnetic forming system.

II. PRINCIPLE OF MAGNETIC FIELD SHAPER

The magnetic field shaper is made of a material of high conductivity with axial slot as shown in Figure 1 [21]. The working principle of the magnetic field shaper can be explained through the current distribution shown in Figure 2. When the capacitor bank of the electromagnetic forming system discharges its stored energy, a pulsed current passes through the driving coil and generates an induced eddy current in the magnetic field shaper. According to the skin effect and Lenz's law, the induced eddy current flows from the axial slot to the outer surface of the magnetic field shaper to form a closed loop. As the excitation source of the workpiece, this current produces an induced eddy current in the workpiece but in the opposite direction of the current in the magnetic field shaper as shown in Figure 2. In this way, the pulse current in the coil is superimposed with the induced eddy current in the magnetic field shaper, and then interacts with the induced eddy current in the workpiece to produce a pulsed electromagnetic force that drives the workpiece to accelerate and deform instantaneously. Because the height of the outer wall of the magnetic field shaper is much smaller than that of the inner wall, and the overall current flowing through both walls is equal, the current density of the outer wall is much higher than that of the inner wall [23]–[25]. This results

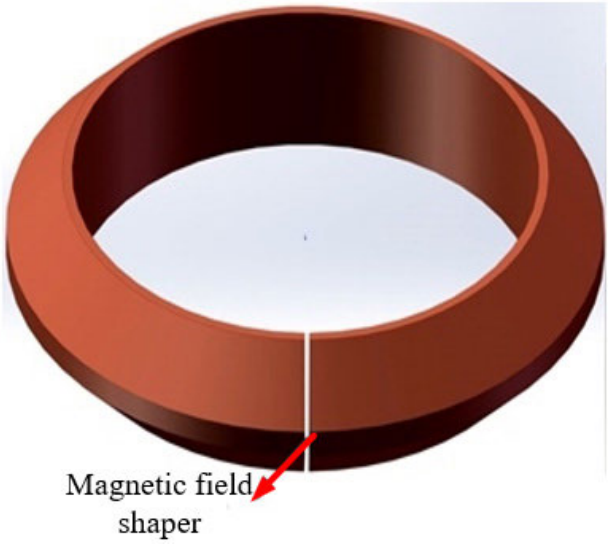

FIGURE 1. Physical structure of the magnetic field shaper [22].

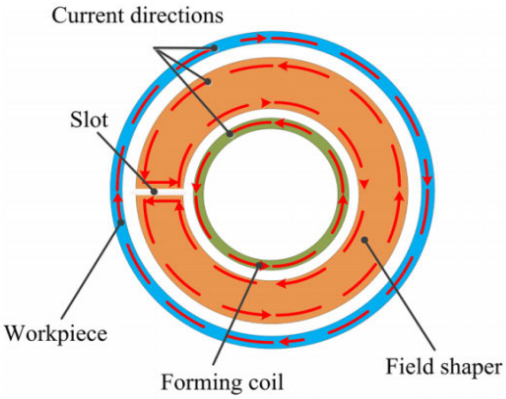

FIGURE 2. Current distribution within the coil, magnetic field shaper and the workpiece.

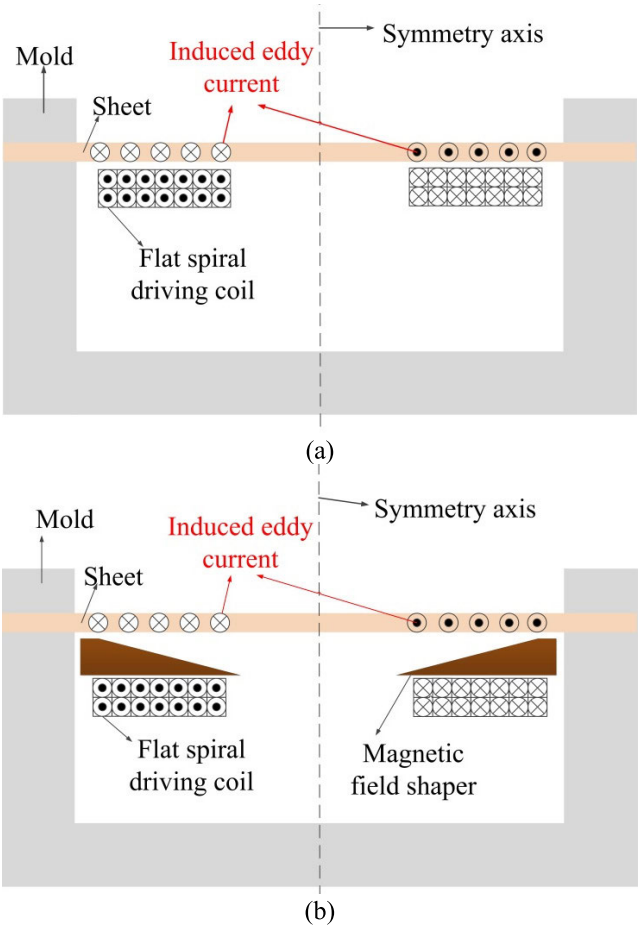

FIGURE 3. Electromagnetic forming system: (a) traditional sheet forming; (b) sheet forming based on the proposed magnetic field shaper.

in strengthening the local electromagnetic force on the workpiece.

The generated electromagnetic force during the forming process can be decomposed into Lorentz axial ($\boldsymbol{F_z}$), and radial ($\boldsymbol{F_r}$) components that can be calculated from the circumferential eddy current $\boldsymbol{J_\varphi}$ and the axial / radial components of the magnetic flux density $\boldsymbol{B_z}$ and $\boldsymbol{B_r}$ as below:

$$\boldsymbol{F_z} = \boldsymbol{J_\varphi} \times \boldsymbol{B_r} \tag{1}$$

$$\boldsymbol{F_r} = \boldsymbol{J_\varphi} \times \boldsymbol{B_z} \tag{2}$$

In the traditional electromagnetic forming process of sheet metals, a single driving coil is usually placed under the sheet, as shown in Figure 3(a). In this method, the radial magnetic flux generated by the driving coil covers the entire sheet, and the peak value of the axial electromagnetic force component appears at about half of the sheet radius. This area has the fastest deformation speed and drives the central area with less constraint to accelerate the deformation. At the end of the process, the middle part of the sheet encounters a large forming amount, while the end part exhibits a smaller amount, which results in uneven radial deformation of the sheet [23], [26], [27]. This drawback can be overcome by

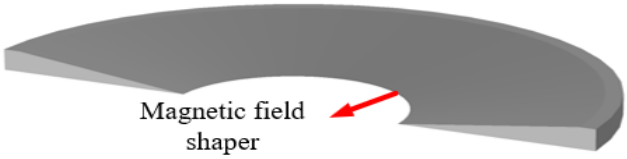

FIGURE 4. Three-dimensional structure diagram of the proposed.

employing the proposed magnetic field shaper, as shown in Figure 3(b). The three-dimensional structure of the proposed magnetic field shaper is shown in Figure 4.

III. ELECTROMAGNETIC-STRUCTURE COUPLING MODEL OF ELECTROMAGNETIC FORMING

In the electromagnetic forming process, the electromagnetic field, structure field and temperature field have strong coupling correlation. A finite element analysis model is developed to simulate this correlation. The finite element electromagnetic-structure 2D coupling model is analyzed, and the effects of workpiece geometry change and deformation speed on circuit, magnetic field and structure field are considered. The coupling between the electric circuit and magnetic field, magnetic field and workpiece deformation is realized to simulate the actual system of thin plate electromagnetic bulging [21]. In [27], the feasibility of replacing the three-dimensional model with a two-dimensional axisymmetric model of the magnetic collector to accelerate the execution time without compromising the model accuracy was verified. Based on this, a two-dimensional axisymmetric model of the electromagnetic forming of sheet metal is established using COMSOL software as per the flow chart of Figure 5. Details of the four modules in this flow chart can be found in [16].

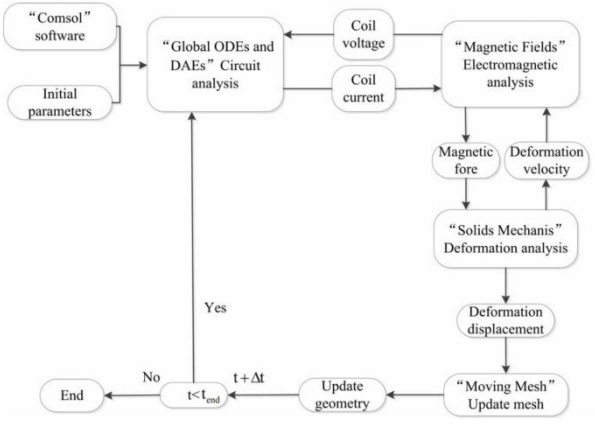

FIGURE 5. Electromagnetic forming simulation flow chart.

The equivalent circuit of traditional sheet metal electromagnetic forming is shown in Figure 6 of which the following equations can be derived based on Kirchhoff's law [23]:

$$\begin{cases} \boldsymbol{U_c} = (R_0 + R)\boldsymbol{I}_{\text{coil}} + (L + L_0)\dfrac{d\boldsymbol{I}_{\text{coil}}}{dt} + M_{m-w}\dfrac{d\boldsymbol{I_w}}{dt} \\ \boldsymbol{U_c} = U_0 - \dfrac{1}{C}\displaystyle\int_0^t \boldsymbol{I}_{\text{c}} dt \end{cases} \tag{3}$$

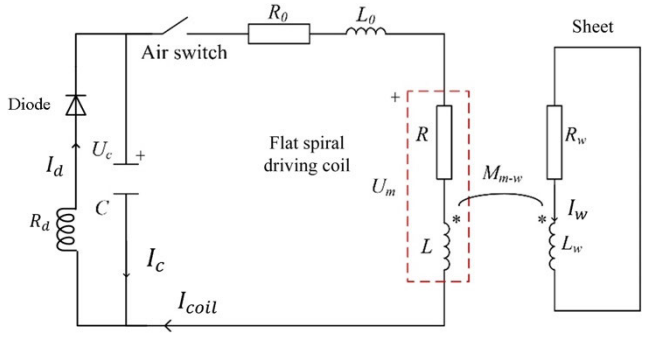

FIGURE 6. Circuit of the traditional sheet electromagnetic forming.

TABLE 1. Circuit parameters.

Symbol	Description	Numerical
C_0	Capacitance	320μF
U_0	Voltage	3.8kV
R_0	Line resistance	25mΩ
L_0	Line inductance	12μH
R_d	Crowbar resistance	0.2Ω
S	Copper wire section	2mmx4mm

$$\begin{cases} \boldsymbol{I}_{\text{coil}} + \boldsymbol{I}_{\text{c}} - \boldsymbol{I}_{\boldsymbol{d}} = 0 \\ R_{\text{w}}\boldsymbol{I}_{\boldsymbol{w}} + L_w \dfrac{d\boldsymbol{I}_{\boldsymbol{w}}}{dt} + M_{w-m}\dfrac{d\boldsymbol{I}_c}{dt} = 0 \end{cases} \tag{4}$$

$$\begin{cases} \boldsymbol{I}_{\boldsymbol{d}} = 0 & U_{\text{c}} \geq 0 \\ \boldsymbol{I}_{\boldsymbol{d}} = \dfrac{\boldsymbol{U}_c}{R_d} & U_{\text{c}} < 0 \end{cases} \tag{5}$$

When the proposed magnetic field shaper is placed between the sheet and the driving coil, the equivalent circuit is modified as shown in Figure 7 [23]. For this circuit, (4) is modified to:

$$\begin{cases} \boldsymbol{I}_{\text{coil}} + \boldsymbol{I}_{\text{c}} - \boldsymbol{I}_{\boldsymbol{d}} = 0 \\ R_f\boldsymbol{I}_f + L_f\dfrac{d\boldsymbol{I}_f}{dt} + M_{f-m}\dfrac{d\boldsymbol{I}_c}{dt} + M_{f-w}\dfrac{d\boldsymbol{I}_w}{dt} = 0 \\ R_{\text{w}}\boldsymbol{I}_{\boldsymbol{w}} + L_w\dfrac{d\boldsymbol{I}_{\boldsymbol{w}}}{dt} + M_{w-f}\dfrac{d\boldsymbol{I}_f}{dt} = 0 \end{cases} \tag{6}$$

where $\boldsymbol{U_C}$ is the voltage across the capacitor with initial value of U_0; $\boldsymbol{I_{coil}}$ is the driving coil current; $\boldsymbol{I_w}$ is the induced eddy current in the sheet; $\boldsymbol{I_f}$ is the eddy current induced in the magnetic field shaper.

Detailed parameters of the equivalent circuit are given in Table 1 while the specific structural parameters are as shown in Figure 8. The upper wall of the magnetic field shaper is 2mm away from the sheet while the lower wall is 2mm away from the coil and the thickness of the magnetic field shaper is 7mm.

The magnetic field shaper module is used to obtain the distribution of the magnetic field and electromagnetic force [28], [29].

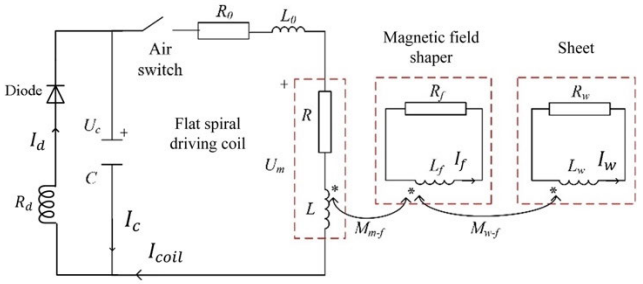

FIGURE 7. Equivalent circuit of sheet electromagnetic forming using a magnetic field shaper.

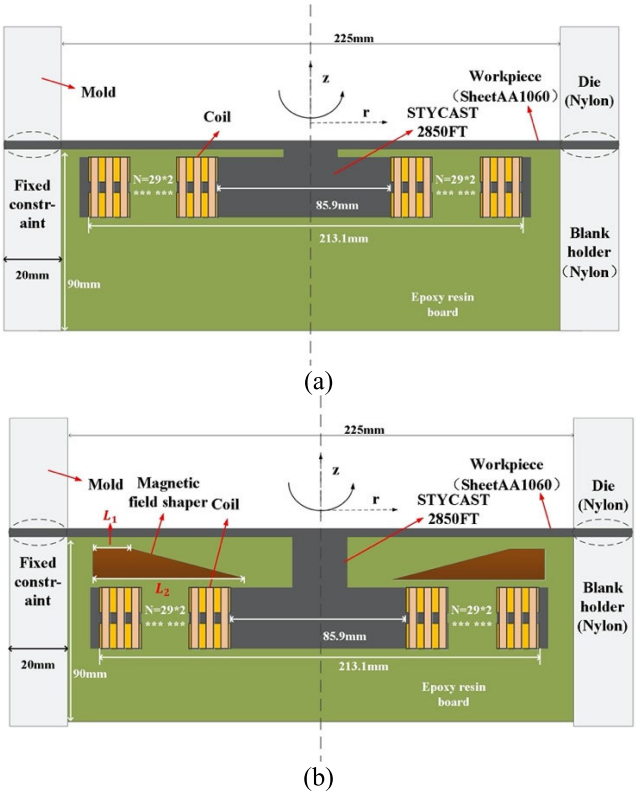

FIGURE 8. Sheet forming dimension drawing: (a) traditional sheet forming; (b) forming of new magnetic field shaper sheet.

The induced eddy current in the workpiece is mainly controlled by the annular component, and can be expressed by Maxwell equation:

$$\nabla \times \boldsymbol{H} = \boldsymbol{J} \tag{7}$$

$$\nabla \times \boldsymbol{E}_{\boldsymbol{\varphi}} = -\frac{\partial \boldsymbol{B}_z}{\partial t} + \nabla \times (\boldsymbol{v}_z \times \boldsymbol{B}_r) \tag{8}$$

$$\nabla \bullet \boldsymbol{B} = 0 \tag{9}$$

$$\boldsymbol{J}_{\boldsymbol{\varphi}} = \frac{\boldsymbol{I}_{coil}}{s} = \gamma \boldsymbol{E}_{\boldsymbol{\varphi}} \tag{10}$$

where $\boldsymbol{E}$ is the electric field intensity, $\boldsymbol{B}$ is the magnetic flux density, $\boldsymbol{v}$ is sheet speed, $\boldsymbol{J}$ is the induced eddy current density, and γ is the sheet conductivity. The subscripts r, φ and z;

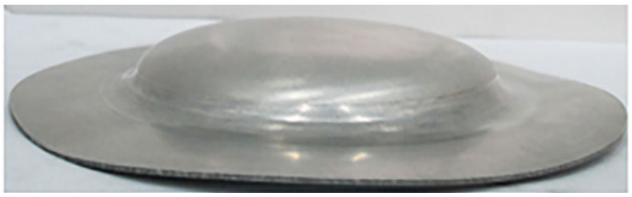

(a)

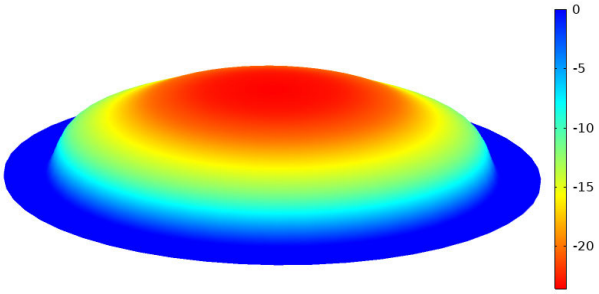

(b)

FIGURE 9. Results of sheet electromagnetic forming: (a) experimental results in [16], (b) simulation results using the proposed finite element model (dimensions are in mm).

represent the radial, circumferential and axial components of the vector, respectively.

When the sheet is stressed, it follows Newton's second law so the relationship between the force and displacement of the sheet is as below:

$$\rho \frac{\partial^2 \boldsymbol{u}}{\partial t^2} - \nabla \bullet \boldsymbol{\sigma} = \boldsymbol{F} \tag{11}$$

where $\boldsymbol{\sigma}$ is the sheet stress tensor, $\boldsymbol{F}$ is the volume density vector of the electromagnetic force, ρ is the sheet density and $\boldsymbol{u}$ is the sheet displacement vector.

In this paper, Cowper-Symonds model with a constitutive equation given by (11) is used to simulate AA1060 sheet.

$$\sigma = [1 + (\frac{\varepsilon_{pe}}{P})^m]\sigma_{ys} \tag{12}$$

where σ_{ys} is the initial yield stress of the sheet, σ is the flow stress when the sheet is deformed at high speed, m is the strain rate hardening parameter, and P is the sheet density. $P = 6500$, $m = 0.25$ are usually used for aluminum [30].

In [16], the electromagnetic forming of a sheet metal loaded by a local coil is investigated through simulation and experimental analyses. Experimental results shown in Figure 9(a) indicate that the final forming of the sheet is almost cylindrical which is in a good agreement with the simulation results shown in Figure 9(b). These results verify the effectiveness of the finite element model used in this paper.

IV. SIMULATION RESULTS

In this section, the influence of the magnetic field shaper geometrical parameters on the electromagnetic force and sheet deformation behavior is studied.

Two structure parameters of the magnetic field shaper are varied in a specific range in order to investigate its impact on the axial electromagnetic force and sheet deformation behavior. These two parameters, shown in Figure 8(b), are L_1 and L_2 which represent the length of the upper and lower wall of the magnetic field shaper; respectively. In the analysis, L_1 is varied in the range 3.5mm to 11.5mm in 2mm steps while maintaining L_2 at 60mm. The effect of L_2 is investigated by changing its value in 2mm steps from 54mm to 66mm while maintaining L_1 at 7.5mm. The interaction of parameters is not considered in the analysis. Other parameters are assumed unchanged and the interaction of other parameters is not considered in the analysis

Figure 10(a) shows the effect of changing L_1 on the axial electromagnetic force. As shown in the Figure, the axial electromagnetic force is concentrated at a sheet radius of 105mm. The peak value of axial electromagnetic force increases with the decrease of L_1, and when L_1 decreases, the peak value of axial electromagnetic force moves slightly toward the end of the sheet.

Figure 10(b) shows the influence of L_1 on the sheet axial deformation. It can be seen that with the increase of L_1, the deformation profile of the sheet changes from convex to flat then to convex again. The relatively flat profile is obtained when L_1 is 7.5mm.

The effect of L_2 variation on the axial electromagnetic force is shown in Figure 11(a). It can be seen that the peak value of the axial electromagnetic force is also at sheet radius of 105mm and the peak value of the axial electromagnetic force decreases with the increase of L_2. In contrary to the effect of L_1, the position of the peak value does not encounter any change with the change of L_2.

Figure 11(b) shows the influence of L_2 on the axial deformation of the sheet. In this case, with the increase of L_2, the deformation profile of the sheet changes from convex to concave, and a relatively flat profile appears when L_2 is 60mm.

The above analysis shows that with a proper structure design of the magnetic field shaper, an optimum sheet deformation can be achieved. It is to be noted that the analysis presented in this paper does not consider the interaction of process parameters. In the investigated case study, the optimum values of L_1 and L_2 of the magnetic field shaper are found to be 7.5mm and 60mm; respectively.

In order to highlight the advantage of the proposed method, a performance comparison with the traditional method is carried out. The geometric parameters of the coils under the two loading methods are given in Table 2. The workpiece is AA1060 aluminum alloy sheet with a diameter of 280mm and a thickness of 2mm. In order to ensure accurate comparison, the forming amount of the two schemes is kept the same by setting different discharge voltages i.e. 1.73kV for the traditional coil method and 3.8kV when the magnetic field shaper is utilized.

In order to illustrate how the sheet forming based on the proposed magnetic field shaper can improve the overall

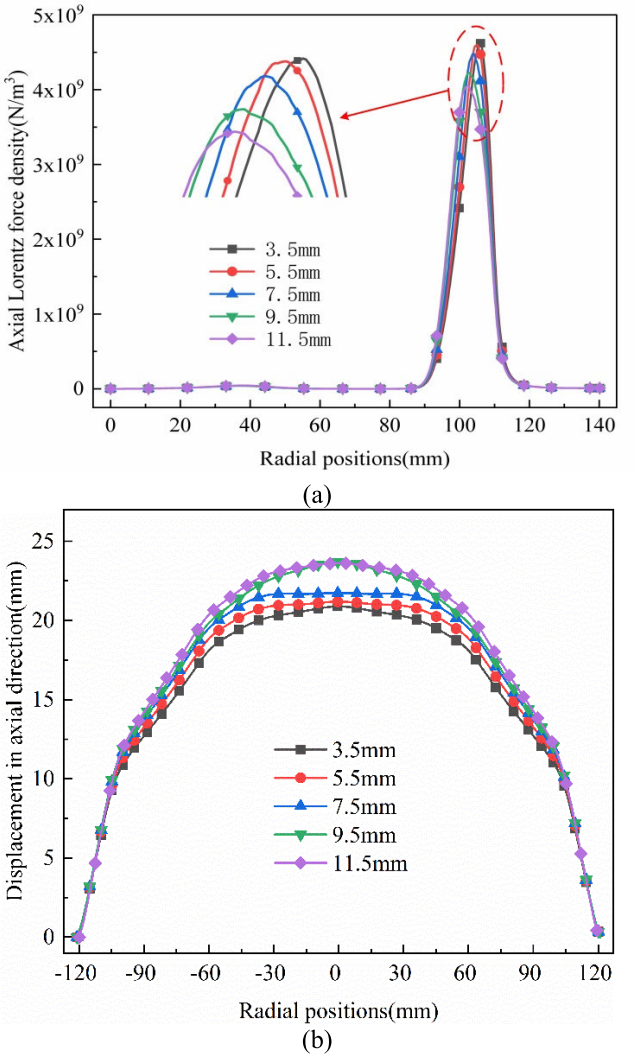

FIGURE 10. Effect of L_1 on the: (a) axial electromagnetic force; (b) deformation behavior.

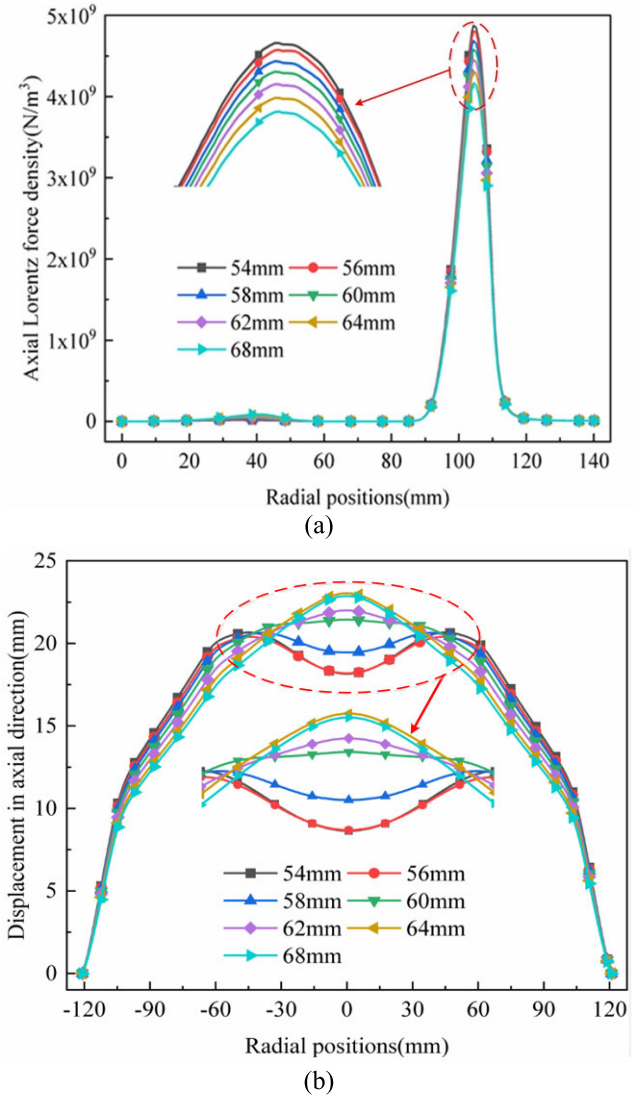

FIGURE 11. Effect of L_2 on the: (a) axial electromagnetic force; (b) deformation behavior.

TABLE 2. Geometric parameters of the coils under the two loading methods (all dimensions are in mm).

		Height	Inner radius	Outer radius
Traditional coil		8.4	43	106.55
With the proposed magnetic field shaper	coil	8.4	43	106.55
	Upper wall		102.5	110
	Lower wall		50	110

uniformity, a three-dimensional plot of the induced eddy current distribution on the upper wall of the sheet with time is shown in Figure 12. When the traditional coil is used for discharging, the induced eddy current is of convex profile, which concentrates at a sheet radius of about 75mm, with a maximum value of $4 \times 10^8\ A/m^2$. When the coil is loaded based on the proposed magnetic field shaper, the induced current is converted into a cone-shape and is distributed along a sheet radius of about 100mm, with a maximum value of $1 \times 10^9\ A/m^2$. In this case, the induced current at the end of the sheet is very large compared to that in the middle and hence the axial electromagnetic force is concentrated at the end, which promotes the deformation of the sheet end, thus improving the forming uniformity of the sheet.

In the sheet electromagnetic forming process, the axial electromagnetic force is determined by the radial magnetic flux component and the induced eddy current. Therefore, the radial magnetic flux density distribution along the radial direction of the sheet is plotted as shown in Figure 13. When a traditional coil is used, the radial magnetic flux exhibits a convex profile and is distributed around a radius of 50mm-100mm. The maximum radial magnetic flux is 1.8T,

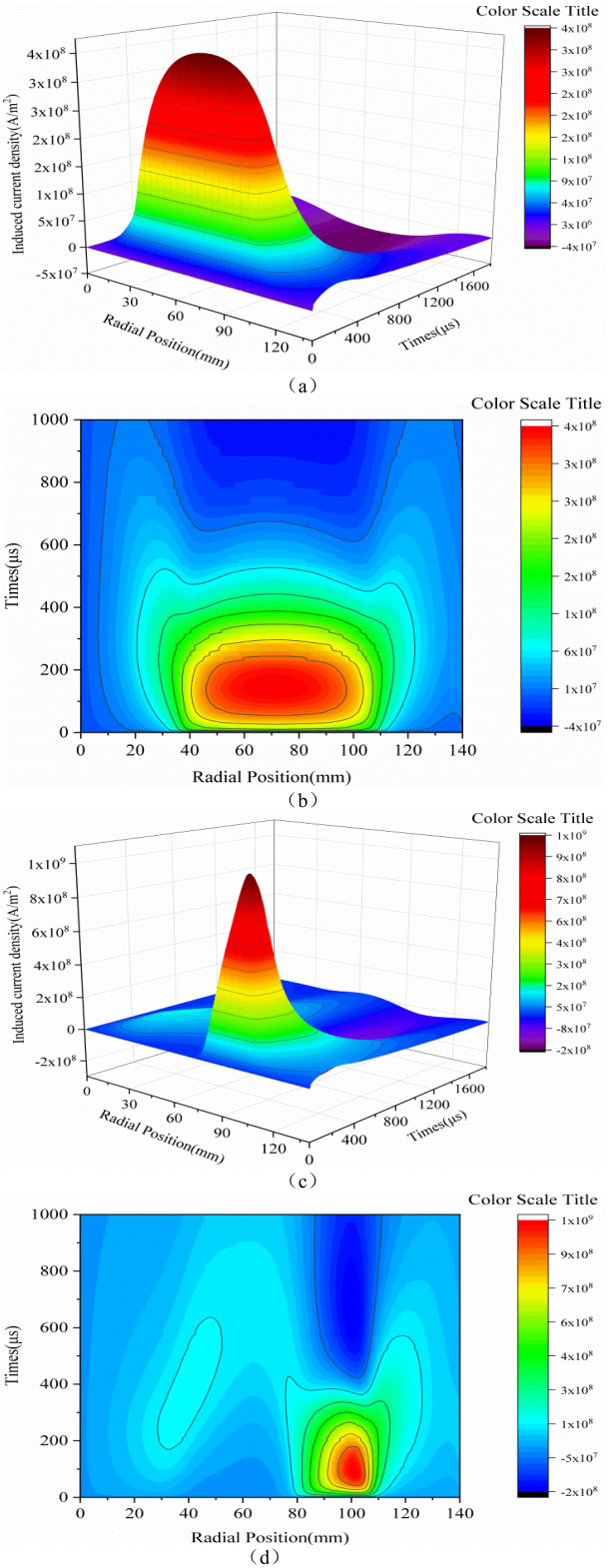

FIGURE 12. Three-dimensional cloud of the induced eddy current distribution with time and radial position. (a) traditional coil, (c) coil loaded by a magnetic field shaper; Top view of (b) traditional coil (d) coil loaded by a magnetic field shaper.

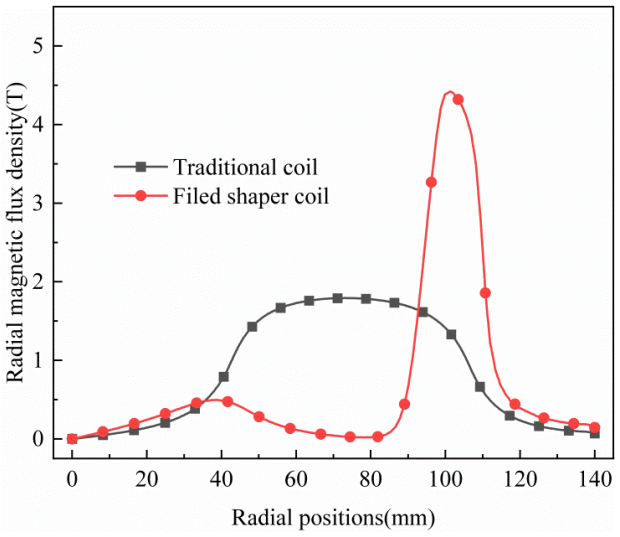

FIGURE 13. Radial distribution of the axial magnetic flux density.

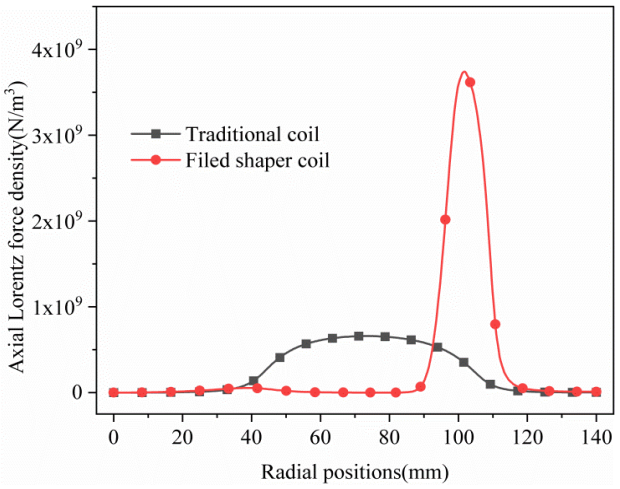

FIGURE 14. Axial distribution the radial electromagnetic force.

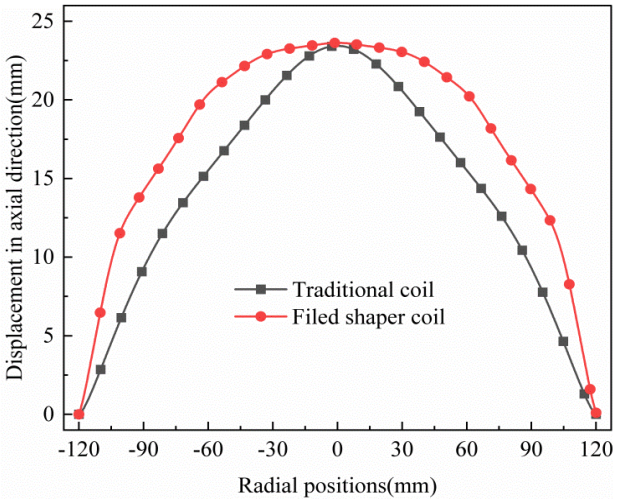

FIGURE 15. Axial deformation of the sheet under the two loading methods.

which is at half of the radius of the sheet. When the proposed magnetic field shaper is employed, the radial magnetic flux is changing to a cone profile which is concentrated at a radius of 105mm, with a maximum value of 4.5T. Figure 14 shows the radial distribution of the axial electromagnetic force on the sheet. Under the traditional method, the axial electromagnetic

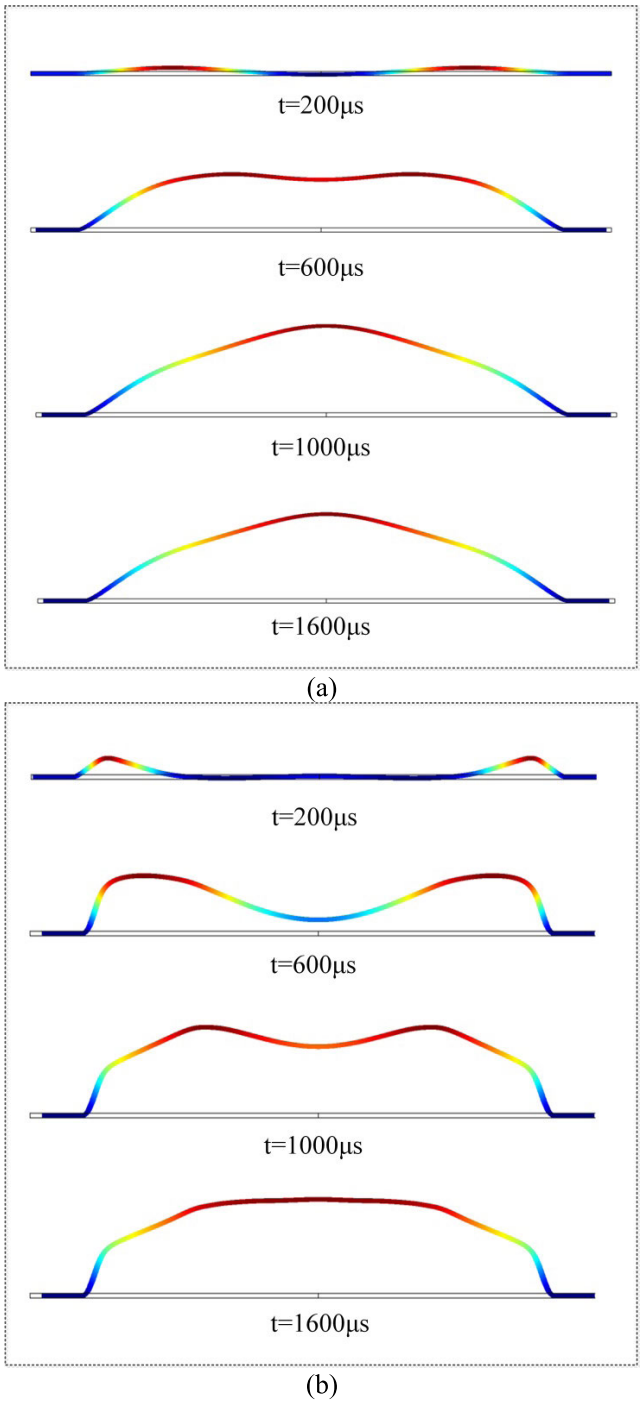

FIGURE 16. Sheet forming conditions at different times: (a) traditional forming, (b) forming based on the proposed magnetic field shaper.

force is distributed in a convex shape, which is distributed around a radius of 50mm-100mm with a peak value of $7.1 \times 10^8\ N/m^3$. With the use of a magnetic field shaper, the axial electromagnetic force is shaped in a conical profile and concentrates at a radius of 100mm with a peak value of $4.8 \times 10^9\ N/m^3$.

Figure 15 shows the axial displacement of the sheet when the traditional coil and the proposed method are used. Under the traditional coil, the radial deformation of the sheet is of

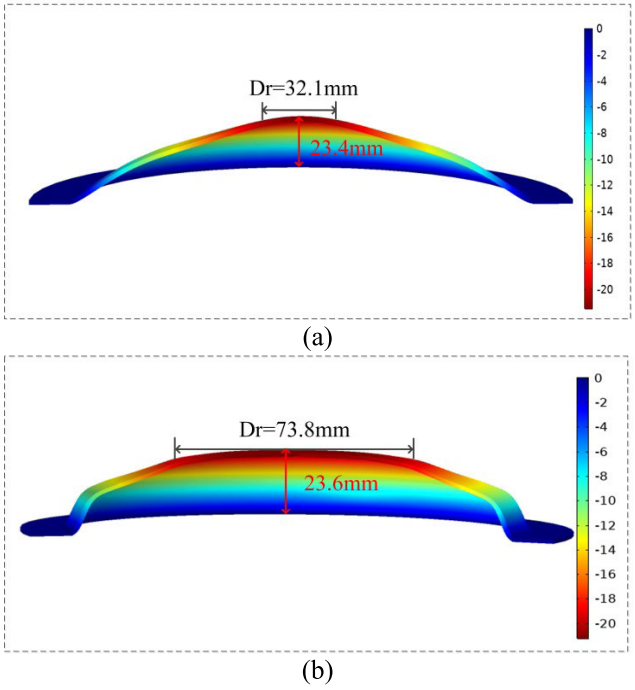

FIGURE 17. Three-dimensional outline drawing of sheet forming: (a) traditional coil; (b) with the proposed magnetic field shaper.

convex profile with a large deformation in the middle of the sheet and small deformation at both ends. Using the magnetic field shaper proposed in this paper, the radial deformation of the sheet becomes evenly distributed in the middle of the sheet and the end effect of the traditional electromagnetic forming is weakened.

In order to better reflect the deformation state of the sheet forming process, the forming states of the sheet under the two loading methods are obtained as shown in Figure 16. It can be seen that at the initial time, t=200μs, when the traditional coil is loaded, the middle part of the sheet starts to deform, while the with the magnetic field shaper deformation starts at the ends of the sheet. At t=1600μs, the maximum deformation of the sheet is achieved. While the radial deformation of the sheet at this instant is uneven and is of convex profile when a traditional coil is loaded, it is uniform when a magnetic field shaper is loaded.

The maximum deformation value D_r of the sheet is defined as the radial length less than or equal to 96% of the maximum deformation level. Figure 17 shows a three-dimensional outline diagram of sheet free forming under the two loading methods. From this figure, $D_r = 32.1$mm when a traditional coil is used. This value increases to 73.8mm when the proposed method is adopted which confirms the superiority of the proposed method over the traditional loading method.

V. CONCLUSION

To solve the problem of uneven radial deformation in traditional sheet electromagnetic forming, this paper proposes an electromagnetic forming technology based on utilizing a magnetic field shaper. Simulation results show that when the

proposed magnetic field shaper is utilized, the axial electromagnetic force is concentrated at the ends of the sheet, while the middle part of the sheet is less affected, which solves the issue of end effect in the traditional forming method. Results also show that there is a specific structural parameter of the magnetic field shaper, which achieves optimum sheet electromagnetic forming uniformity. The scheme proposed in this paper can effectively change the distribution of the induced eddy current in the sheet, and concentrate the magnetic flux density and electromagnetic force at both ends of the sheet. When the axial forming amount of the sheet is kept the same, compared with the traditional coil loading, the coil loading based on the proposed magnetic field shaper improves the uniformity of the sheet, and the maximum uniform deformation area increases from 32.1mm to 73.8mm. However, using the magnetic field shaper calls for higher discharge voltage and the process efficiency will be reduced. Future experimental analysis is essential to validate the simulation results obtained in this paper. Also, further research is required to optimize the process efficiency while reducing the discharge voltage when a magnetic field shaper is used.

REFERENCES

[1] L. Qiu, K. Deng, Y. Li, X. Tian, Q. Xiong, P. Chang, P. Su, and L. Huang, "Analysis of coil temperature rise in electromagnetic forming with coupled cooling method," *Int. J. Appl. Electromagn. Mech.*, vol. 63, no. 1, pp. 45–58, May 2020, doi: 10.3233/JAE-190062.

[2] Y. Y. Chu, R. S. Lee, V. Psyk, and A. E. Tekkaya, "Determination of the flow curve at high strain rates using electromagnetic punch stretching," *J. Mater. Process. Technol.*, vol. 212, no. 6, pp. 1314–1323, Jun. 2012.

[3] Q. Cao, L. Du, Z. Li, Z. Lai, Z. Li, M. Chen, X. Li, S. Xu, Q. Chen, X. Han, and L. Li, "Investigation of the Lorentz-force-driven sheet metal stamping process for cylindrical cup forming," *J. Mater. Process. Technol.*, vol. 271, pp. 532–541, Sep. 2019.

[4] L. Qiu, C. Wang, A. Abu-Siada, Q. Xiong, W. Zhang, B. Wang, N. Yi, Y. Li, and Q. Cao, "Coil temperature rise and workpiece forming efficiency of electromagnetic forming based on half-wave current method," *IEEE Access*, vol. 8, pp. 9371–9379, 2020, doi: 10.1109/ACCESS.2020.2965254.

[5] S. Ouyang, X. Li, C. Li, L. Du, T. Peng, X. Han, L. Li, Z. Lai, and Q. Cao, "Investigation of the electromagnetic attractive forming utilizing a dual-coil system for tube bulging," *J. Manuf. Processes*, vol. 49, pp. 102–115, Jan. 2020.

[6] L. Qiu, N. Yi, A. Abu-Siada, J. Tian, Y. Fan, K. Deng, Q. Xiong, and J. Jiang, "Electromagnetic force distribution and forming performance in electromagnetic forming with discretely driven rings," *IEEE Access*, vol. 8, pp. 16166–16173, 2020, doi: 10.1109/ACCESS.2020.2967096.

[7] M. Geier, E. Paese, R. Rossi, P. A. R. Rosa, and R. P. Homrich, "Experimental analysis of interference-fit joining of aluminum tubes by electromagnetic forming," *IEEE Trans. Appl. Supercond.*, vol. 30, no. 4, pp. 1–6, Jun. 2020, doi: 10.1109/TASC.2020.2972499.

[8] L. Qiu, W. Zhang, A. Abu-Siada, Q. Xiong, C. Wang, Y. Xiao, B. Wang, Y. Li, J. Jiang, and Q. Cao, "Electromagnetic force distribution and wall thickness reduction of three-coil electromagnetic tube bulging with axial compression," *IEEE Access*, vol. 8, pp. 21665–21675, 2020. 10.1109/ACCESS.2020.2969678

[9] S. Golowin, M. Kamal, J. Shang, J. Portier, A. Din, G. S. Daehn, J. R. Bradley, K. E. Newman, and S. Hatkevich, "Application of a uniform pressure actuator for electromagnetic processing of sheet metal," *J. Mater. Eng. Perform.*, vol. 16, no. 4, pp. 455–460, Aug. 2007.

[10] L. Qiu, Y. Yu, Q. Xiong, C. Deng, Q. Cao, X. Han, and L. Li, "Analysis of electromagnetic force and deformation behavior in electromagnetic tube expansion with concave coil based on finite element method," *IEEE Trans. Appl. Supercond.*, vol. 28, no. 3, Apr. 2018, Art. no. 0600705, doi: 10.1109/TASC.2017.2789287.

[11] L. Qiu, W. Zhang, A. Abu-Siada, G. Liu, C. Wang, Y. Wang, B. Wang, Y. Li, and Y. Yu, "Analysis of electromagnetic force and formability of tube electromagnetic bulging based on convex coil," *IEEE Access*, vol. 8, pp. 33215–33222, 2020, doi: 10.1109/ACCESS.2020.2974758.

[12] L. Qiu, Y. Li, Y. Yu, A. Abu-Siada, Q. Xiong, X. Li, L. Li, P. Su, and Q. Cao, "Electromagnetic force distribution and deformation homogeneity of electromagnetic tube expansion with a new concave coil structure," *IEEE Access*, vol. 7, pp. 117107–117114, 2019.

[13] Z. Jian *et al.*, "Numerical simulation and forming uniformity of electromagnetic progressive bulging of tube," *J. Plasticity Eng.*, vol. 19, no. 5, pp. 92–99, 2012.

[14] L. Qiu, C. Wang, A. Abu-Siada, W. Bin, Z. Wang, W. Ge, C. Liu, and P. Chang, "Parametric simulation analysis of the electromagnetic force distribution and formability of tube electromagnetic bulging based on auxiliary coil," *IEEE Access*, vol. 8, pp. 159979–159989, 2020. 10.1109/ACCESS.2020.3020830

[15] M. Kamal and G. S. Daehn, "A uniform pressure electromagnetic actuator for forming flat sheets," *J. Manuf. Sci. Eng.*, vol. 129, no. 2, p. 369, Jan. 2007.

[16] M. Geier, M. M. José, R. Rossi, P. A. R. Rosa, and P. A. F. Martins, "Interference-fit joining of aluminium tubes by electromagnetic forming," *Adv. Mater. Res.*, vol. 853, pp. 488–493, Dec. 2013.

[17] L. Qiu, Y. Yu, Y. Yang, X. Nie, Y. Xiao, Y. Ning, F. Wang, and C. Cao, "Analysis of electromagnetic force and experiments in electromagnetic forming with local loading," *Int. J. Appl. Electromagn. Mech.*, vol. 57, no. 1, pp. 29–37, Apr. 2018.

[18] M. A. Bahmani, K. Niayesh, and A. Karimi, "3D simulation of magnetic field distribution in electromagnetic forming systems with field-shaper," *J. Mater. Process. Technol.*, vol. 209, no. 5, pp. 2295–2301, Mar. 2009.

[19] D. S. K, M. R. Kulkarni, S. Kumar, P. C. Saroj, and A. Sharma, "Magnetic field enhancement using field shaper for electromagnetic welding system," in *Proc. IEEE Appl. Electromagn. Conf. (AEMC)*, Dec. 2015, pp. 1–2.

[20] H. Suzuki, M. Murata, and H. Negishi, "The effect of a field shaper in electromagnetic tube bulging," *J. Mech. Work. Technol.*, vol. 15, no. 2, pp. 229–240, Sep. 1987.

[21] L. Qiu, C. Wang, A. Abu-Siada, W. Bin, Z. Wang, W. Ge, C. Liu, and Y. Fan, "Numerical analysis of tube expansion by electromagnetic forming using magnetic field shaper," *IEEE Access*, vol. 8, pp. 196253–196263, 2020, doi: 10.1109/ACCESS.2020.3033622.

[22] P. Gharghabi, P. Dordizadeh, and K. Niayesh, "Impact of metal thickness and field shaper on the time-varying processes during impulse electromagnetic forming in tubular geometries," *J. Korean Phys. Soc.*, vol. 59, no. 6, pp. 3560–3566, 2011.

[23] E. Paese, M. Geier, R. P. Homrich, R. Rossi, and P. A. R. C. Rosa, "Parametric study of the design variables involved in the EMF process of sheet metal," *IEEE Trans. Appl. Supercond.*, vol. 30, no. 4, pp. 1–6, Jun. 2020.

[24] W. Luo, L. Huang, J. Li, X. Liu, and Z. Wang, "A novel multi-layer coil for a large and thick-walled component by electromagnetic forming," *J. Mater. Process. Technol.*, vol. 214, no. 11, pp. 2811–2819, Nov. 2014.

[25] H. A. Wheeler, "Formulas for the skin effect," *Proc. IRE*, vol. 30, no. 9, pp. 412–424, Sep. 1942.

[26] E. Paese, P. A. R. Rosa, M. Geier, R. P. Homrich, and R. Rossi, "An analysis of electromagnetic sheet metal forming process," *Appl. Mech. Mater.*, vol. 526, pp. 9–14, Feb. 2014.

[27] N. Takatsu, M. Kato, K. Sato, and T. Tobe, "High-speed forming of metal sheets by electromagnetic force," *JSME Int. J. Vib., Control Eng., Eng. Ind.*, vol. 31, no. 1, pp. 142–148, 1988.

[28] L. Qiu, K. Deng, A. Abu-Siada, Q. Xiong, N. Yi, Y. Fan, J. Tian, and J. Jiang, "Construction and analysis of two-dimensional axisymmetric model of electromagnetic tube bulging with field shaper," *IEEE Access*, vol. 8, pp. 113713–113719, 2020, doi: 10.1109/ACCESS.2020.3003740.

[29] L. Du, L. Xia, X. Li, L. Qiu, Z. Lai, Q. Chen, Q. Cao, X. Han, and L. Li, "Adjustable current waveform via altering the damping coefficient: A new way to reduce joule heating in electromagnetic forming coils," *J. Mater. Process. Technol.*, vol. 293, Jul. 2021, Art. no. 117086.

[30] X. Zhang, Q. Cao, X. Han, Q. Chen, Z. Lai, Q. Xiong, F. Deng, and L. Li, "Application of triple-coil system for improving deformation depth of tube in electromagnetic forming," *IEEE Trans. Appl. Supercond.*, vol. 26, no. 4, pp. 1–4, Jun. 2016, doi: 10.1109/TASC.2016.2542482.

[31] L. Qiu, B. Wang, A. Abu-Siada, Q. Xiong, W. Zhang, W. Ge, C. Liu, L. Jiang, and C. Wang, "Research on forming efficiency in double-sheet electromagnetic forming process," *IEEE Access*, vol. 8, pp. 19248–19255, 2020, doi: 10.1109/ACCESS.2020.2968049.

LI QIU (Member, IEEE) received the B.S., M.S., and Ph.D. degrees in electrical engineering from the Huazhong University of Science and Technology, Wuhan, China in 2012. He is currently an Associate Professor with the College of Electrical Engineering and New Energy, China Three Gorges University, Yichang. He is the author of more than 15 articles, and more than ten inventions. His research interests include the technology of pulsed high magnetic field, high voltage technology, and electromagnetic forming. He is a Periodical Reviewer of IEEE TRANSACTIONS ON APPLIED SUPERCONDUCTIVITY and the *International Journal of Applied Electromagnetics and Mechanics*.

WEIYE WU is currently pursuing the degree in electrical engineering with the College of Electrical Engineering and New Energy, China Three Gorges University, Yichang.

AHMED ABU-SIADA (Senior Member, IEEE) received the B.Sc. and M.Sc. degrees in electrical engineering from Ain Shams University, Egypt, in 1998, and the Ph.D. degree in electrical engineering from Curtin University, Australia, in 2004. He is currently an Associate Professor and the Discipline Lead of the Electrical and Computer Engineering, Curtin University. His research interests include power electronics, power system stability, condition monitoring, and power quality. He is the Vice-Chair of the IEEE Computation Intelligence Society, WA Chapter. He is the Editor-in-Chief of the *International Journal of Electrical and Electronics Engineering* and a Regular Reviewer for various IEEE TRANSACTIONS.

BIN WANG is currently pursuing the degree in electrical engineering with the College of Electrical Engineering and New Energy, China Three Gorges University, Yichang.

WANG ZHANG is currently pursuing the degree in electrical engineering with the College of Electrical Engineering and New Energy, China Three Gorges University, Yichang.

XI TIAN is currently pursuing the degree in electrical engineering with the College of Electrical Engineering and New Energy, China Three Gorges University, Yichang.

CHENGLIN WANG was born in Sichuan, China, in 1996. He received the bachelor's degree from the College of Information Science and Engineering, Chengdu University, Chengdu, China, in 2019. He is currently a Graduate Student majoring in electrical engineering with the College of Electrical Engineering and New Energy, China Three Gorges University, Yichang.